Molecular Dynamics Studies on the Structure of Binary Metallic Glasses based on Lennard-Jones (12-6) Potentials

I. $Ni_{81}B_{19}$ and $Cu_{57}Zr_{43}$

O. Beyer and C. Hoheisel
Lehrstuhl für Theoretische Chemie, Ruhr-Universität Bochum

Z. Naturforsch. **38 a**, 859–865 (1983); received February 19, 1983

For the metallic glass $Ni_{81}B_{19}$ the partial pair-distribution functions are determind up to 14 Å by a molecular dynamics simulation using effective Lennard-Jones potentials. The obtained pair-distribution functions are in good agreement with the measured ones. As the simulation was carried out at the thermodynamic conditions for a liquid, we conclude that the characteristic features of the structure of the metallic glass are essentially not different from those of the fluid system $Ni_{81}B_{19}$ at high temperature and pressure. Both the high reduced density of the system and the large differences in the atomic radii of the two species dominantly determine the form of the partial structure factors of the glass. These findings have been confirmed by our molecular dynamics simulation of a further metallic glass, the $Cu_{57}Zr_{43}$ system.

1. Introduction

Studies on the structure of binary metallic glasses have lately found increasing interest [1, 2, 3] because of the usefulness of these substances for practical purposes [4]. Though the determination of the partial structure-factors is difficult [3, 5], modern x-ray and neutron-scattering experiments enable experimentalists to evaluate them with sufficient accuracy [6, 7]. Simultanously with the improvement of the scattering experiments, approaches have been made to predict the structure of these glasses [8]. Most of the theoretical work is done in terms of model-calculations, using hard-sphere or micro-cluster or relaxation models [9, 10, 11]. We hope to show that molecular dynamics simulations can contribute valuable information about the structure of binary metallic glasses. The systems chosen are $Ni_{81}B_{19}$ and $Cu_{57}Zr_{43}$. Whereas the pair-distribution functions of the former were reliably measured by Steeb *et al.* [12, 13], the existing experimental results on the distribution functions of the latter are not consistent [5, 14, 15].

2. Method and interaction potential

The simulation of molecular dynamics (MD) is now well established and its principles must not be reported here [16, 17, 18]. MD has mostly been applied to simple liquids and dense fluids, for which the interparticle-potential is represented by a Lennard-Jones (12-6) potential

$$u(r)=4\varepsilon\left[\left(\frac{\sigma}{r}\right)^{12}-\left(\frac{\sigma}{r}\right)^{6}\right]\begin{cases}-\varepsilon = \text{minimum value of } u\,,\\ \sigma = \text{distance at } u=0\,.\end{cases}$$

The densities and temperatures of these systems lie mostly in the range of

$$0.80 < T^* < 1.2\,; \quad 0.70 < \varrho^* < 1.0\,,$$

where $T^* = kT/\varepsilon$ and $\varrho^* = (N/V)\sigma^3$ are reduced parameters and N/V is the number density. For binary mixtures the following generalization of the reduced parameters is commonly used [16, 19]:

$$T^* = kT/\varepsilon_x\,; \quad \varrho^* = (N/V)\sigma_x^3\,.$$

Here σ_x, ε_x are defined by the mixing rules

$$\sigma_x^3 = x_1^2\sigma_{11}^3 + 2x_1x_2\sigma_{12}^3 + x_2^2\sigma_{22}^3\,,$$
$$\varepsilon_x\sigma_x^3 = x_1^2\varepsilon_{11}\sigma_{11}^3 + 2x_1x_2\varepsilon_{12}\sigma_{12}^3 + x_2^2\varepsilon_{22}\sigma_{22}^3\,.$$

The subscripts 1 and 2 refer to the components of the mixture and the x_i denote the mole fractions. The ε_{12}, σ_{12} parameters are often generated by the Lorentz-Berthelot (L-B) *combination rules* (see below). Our concept of treating a metallic glass as a fluid bears two essential difficulties: (i) The applicability of effective Lennard-Jones (L-J) pair-potentials for metallic glasses is questionable and (ii) for metals the attractive part of the effective potential

Reprint requests to Dr. C. Hoheisel, Ruhr-Universität, Theoretische Chemie, Postfach 10 21 48, 4630 Bochum 1.

0340-4811 / 83 / 0800-0859 $ 01.3 0/0. – Please order a reprint rather than making your own copy.

and the reduced density of these substances are very high compared to normal liquids.

Whereas for the simulation of, say, the liquid mixture Ar/Kr the ε_{11}, ε_{22}, ε_{12} vary between 100 and 200 K (in multiples of the Boltzmann constant) the absolute ε_{ik}-values for the binary glass Cu/Zr range from 5000 to 8000 K.

Furthermore, the reduced density of the glasses lies between 1.0 and 1.4, so that the particles are not far from close-packed in the sense of the comparable hard-sphere system. MD on these systems for temperatures near room-temperature, i.e. at $T^* = 0.05$, would not lead to any meaningful result, since the system would not approach the thermodynamic equilibrium [20, 21]. However, in our opinion, the structure of the glass is primarily characterized by that of a binary alloy at thermodynamic equilibrium, that is at much higher temperatures. Consequently we performed our calculations actually at reduced temperatures of $T^* \approx 1$. In other words, all our simulations were done on a "Lennard-Jones fluid" at commonly used reduced values of temperature, but at larger densities. It turned out that the relatively high reduced densities ranging from 1.0 to 1.4 lead to pressures of some kilo- or mega-bars, but otherwise have no effect on the convergence of the MD, i.e. the course of the system to an equilibrium-state.

This extreme increase of the pressure has to be expected since the mean distance of the particles amounts to about one σ-unit, so that the steep repulsive part of the potential becomes predominant. On Table 1, we list the peak-positions of the mean peak of the pair-distribution functions of the Ni/B system together with the corresponding σ_{ij}-value of the potential function. On comparing these values, it appears evident that the nearest neighbours are situated deeply in the repulsive part of the potential function. In contrast, the mean distances of particles of normal liquids lie within the range of the minimum of the potential [22].

Table 2. Technical details of the MD-runs.

	$Ni_{81}B_{19}$	$Cu_{57}Zr_{43}$
Particle number	2048	2048
Cut-off-radius	2.5 σ_{ij}-units	2.5 σ_{ij}-units
Time-step	$1.7 \cdot 10^{-15}$ s	$3.3 \cdot 10^{-15}$ s
Equilibration	3900 steps	2900 steps
At equilibrium	2100 steps	2100 steps
Box lengths	27.95 Å	32.45 Å
Computation time (Cyber 205-vector-processor)	0.6 s/step	0.6 s/step

Apart from this effect of a particularly high pressure, the MD shows its usual behaviour. The temperature fluctuations are relatively not greater than for "normal" MD-systems. The average drift of the mean temperature was 0.3% of the final equilibrium value and the total energy was conserved to 0.01% of the final kinetic energy. Other technical details of the MD-runs are given in Table 2.

3. The system $Ni_{81}B_{19}$

It seems intuitively clear that a binary metallic glass has a much more complicated structure than a binary liquid of simple, spherically symmetric particles, as for instance the Ar/Kr mixture. Our conception of treating a metallic glass as a liquid in thermodynamic equilibrium will therefore only be reasonable if the applied potential parameters of the L-J pseudo-potentials are allowed to be varied in a larger range than those describing real liquids.

Whilst for liquid mixtures the Lennard-Jones parameters of the individual kind of particles are practically not different from those of the pure substances, significant deviations are expected for metallic glasses. Particularly, the potential-parameters for the unlike interactions shall not obey the commonly used combining rules of the Berthelot-Lorentz type

$$\sigma_{12} = \tfrac{1}{2}(\sigma_{11} + \sigma_{22}), \quad \varepsilon_{12} = (\varepsilon_{11} \cdot \varepsilon_{22})^{1/2}.$$

Table 1. The The $Ni_{81}B_{19}$-system: The L-J-parameters, the positions of the first peaks and the atomic diameters (experimental data from [13], crystal data from [31] and [32]).

	ε_{ij}/K	σ_{ij}/Å	r_{ij}^{theo}/Å	r_{ij}^{exp}/Å	d^{theo}/Å	d^{exp}/Å	d^{crys}/Å
Ni-Ni	5985.6	2.584	2.51	2.53	2.51	2.53	2.49
Ni-B	6694.6	2.085	2.10	2.11	–	–	–
B-B	7487.8	2.886	3.26	3.28	1.69	1.69	1.589–1.76

Nevertheless, using the Lennard-Jones σ_{ii}-parameters as adjustable parameters in this general sense and leaving the ε_{ii} unchanged, we are enabled to show that MD reproduces the experimental structure factors fairly well. No specific micro-cluster-model has to be employed.

We started our computations by simultating the system $Ni_{81}B_{19}$.

This alloy exhibits by no means an easily interpretable structure. However, in view of the very accurate experimental investigations on the partial radial pair-distribution functions of this Ni/B system, we have chosen this mixture to base our calculations on reliable experimental data.

The interesting feature of the $Ni_{81}B_{19}$ system is a surprising sharpness of the B-B pair-distribution function (PDF), which ranges up to 12 Å and is comparable to that of the Ni-Ni distribution. This indicates that the structure of the Ni/B system deviates appreciably from that of normal liquids. In norml liquids the PDF of the smaller sized particles should undergo a faster decay than that of the larger particles. Moreover, the first peak of the smaller particles should appear at a shorter distance than that of the other species. Though in the case of the Ni/B glass the boron-radius is known to be by a factor of 1.5 smaller than the Ni-atom-radius, at least as far as data of crystals or chemical compounds are concerned, the reverse is here in fact true, as the measurements indicate: the B-B main peak occurs at a somewhat higher r-value than the corresponding Ni-Ni peak.

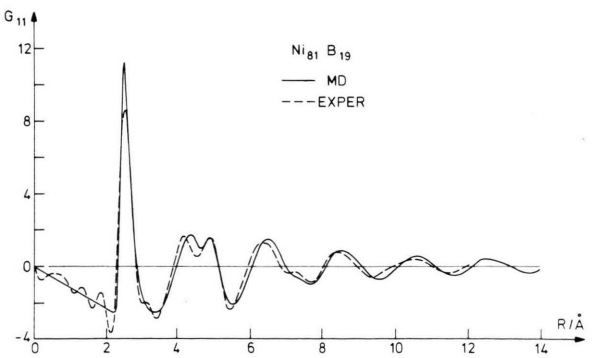

Fig. 1. Reduced partial pair-distribution function $G_{Ni\text{-}Ni}(R)$ of the system $Ni_{81}B_{19}$ in units of $Å^{-2}$ (The linear part before the first peak in the MD-curve indicates that the radial pair-distribution function $g_{Ni\text{-}Ni}(R)$ is here exactly zero; Experimental data from [13]).

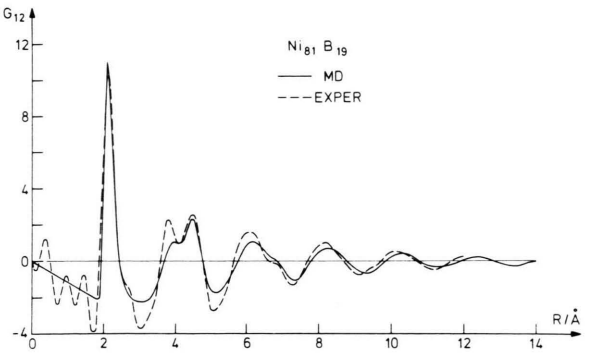

Fig. 2. As in Fig. 1, but $G_{Ni\text{-}B}(R)$.

If despite of this, potential functions commonly used for liquids are to be applied to the Ni/B glass the B-B interaction has to be described by an artificially enlarged effective radius, whereas the other interactions, Ni-B and Ni-Ni correspond nearly to their values known from crystal data.

A comparison of the atomic diameters obtained from crystal- and molecule-data and those roughly estimated from the first peaks of the partial PDF supports our prediction, see Table 1. Whilst the σ-parameters of Ni-Ni and Ni-B fall in line with the numbers evaluated from the PDF's, the B-B parameter is found to disagree strongly. The objection that the first visible line of the B-B PDF might be the second peak, and the first peak has possible disappeared, is not acceptable in view of the sharpness of the B-B PDF and its "long-range" character.

We adjusted therefore the $\sigma_{B\text{-}B}$-parameter to reproduce the first peak of the experimental G_{22}-curve (the subscript 2 always refers to B) and left the other prameters essentially unchanged. Pilot MD-runs were done with systems of 256 and 500 particles at the experimentally evaluated density. These calculations generated the final optimized σ_{ij}-parameters listed on Table 1. To obtain the G_{ij} function in a sufficiently large range of 10 – 15 Å, we used a big system of 2048 particles. The pair-correlation functions are reliably accessible from MD up to only half the length of the periodic box [16]. For a 2048-particle-system the box-length amounts to 28 Å at a density of 8.4 g/cm^3, which suffices for the determination of the PDF up to 14 Å.

The results of these computations are displayed on the Figs. 1 – 3, where our calculated partial G_{ij} function are directly plotted against the experimen-

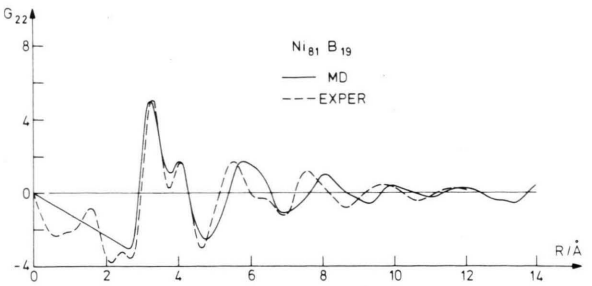

Fig. 3. As in Fig. 1, but $G_{B\text{-}B}(R)$.

tally determind curves [13]. In view of the rather simplified Lennard-Jones model the agreement between the theoretical and the experimental curve appears to be fairly good (see also Appendix).

As expected, the Ni-Ni and Ni-B PDF's show only slight deviations from the experimental curves, whereas the B-B PDF differs noticeably for the higher order peaks. The positions of the calculated peaks exceed those of the experimental ones, and the form of the theoretical peaks is less structured than that of the measured ones. The latter effect naturally follows from the spherically symmetric pseudo-potential used in the simulations, which is surely an insufficient approximation for the "realistic" B-B interaction, particularly due to the fact that we have used an artificially enlarged σ_{BB}-parameter, see Section 6.

4. The $Cu_{57}Zr_{43}$ system

In contrast to the Ni/B system, the $Cu_{57}Zr_{43}$ metallic glass is experimentally not confidently investigated [14, 15].

There are measurements of a few authors, which report contradictory PDF's as far as the position and the height of the peaks is concerned. Moreover, the density of this system is not unambiguously known from experiment [23, 24]. There exist theoretical PDF's calculated by relaxation methods, but the first peaks of these functions are much higher than the experimental ones [25, 26].

With regard to this situation our attempt to simulate the Cu/Zr system has an unsafe basis. Consequently our finally obtained G_{ij}-functions can deviate in detail from accurately measured G_{ij}-curves, but the main features of the structure of the Cu/Zr-system is presumably predicted well by our MD. This can be claimed due to the following reasons:

The Cu/Zr system involves atoms of not too unequal size. That is, the ratio σ_{22}/σ_{11} [33] of the pseudo-L-J-potentials of Zr and Cu (Cu is marked by the index 1) amounts to 1.24 compared to 1.63 for the Ni/B-system.

Table 3 lists these parameters as available from crystal data [27, 28]. As furthermore the 1−2 interaction of these atoms is known to deviate not appreciably from the L-B estimate [5, 14, 16], the structure of this alloy is mainly governed by the density and not by the different size of the component particles nor by an anomalous 1−2 potential parameter. Note that in fluids the σ_{22}/σ_{11} ratio characterizes the structure of the pair-correlation functions [29, 30].

The reduced density of the Cu/Zr system resembles that of real liquids and therefore any particular structure of the partial PDF's is not expected. Note that the reduced density of the Ni/B glass exceeds that of Cu/Zr by more than 30% (see Table 4).

The Figs. 4, 5 and 6 contain the plots of simulated G_{ij}-functions based on the listed σ_{ij} and ε_{ij} parameters. Two densities have been probed according to the experimental uncertainty of this quantity. However, the effect on the final G_{ij}-functions was found to be very small. This has to be ascribed to the low absolute value of ϱ^* compared to that of the Ni/B system. As the available experimental G_{ij}-curves [5, 14, 15] seem unreliable, we have restrained from adding these functions on the Figures 4−6. On the

Table 3. L-J-parameters for the $Cu_{57}Zr_{43}$-systems from crystal data (see Appendix; k Boltzmann constant).

	ε_{ij}/k	σ_{ij}
Cu-Cu	4743.6 K	2.340 Å
Cu-Zr	6365.0 K	2.625 Å
Zr-Zr	8540.7 K	2.910 Å

Table 4. Densities used for MD.

	ϱ/g cm^{-3}	ϱ^*
$Ni_{81}B_{19}$	8.4	1.404
$Cu_{57}Zr_{43}$	7.51	1.054

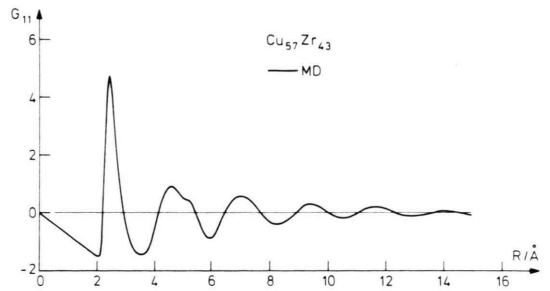

Fig. 4. Reduced partial pair-distribution function $G_{\text{Cu-Cu}}(R)$ of the model-system $Cu_{57}Zr_{43}$ in units of $Å^{-2}$.

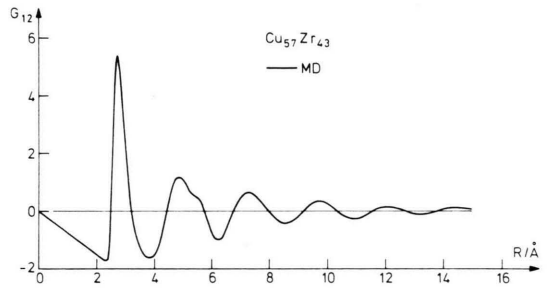

Fig. 5. As in Fig. 4, but $G_{\text{Cu-Zr}}(R)$.

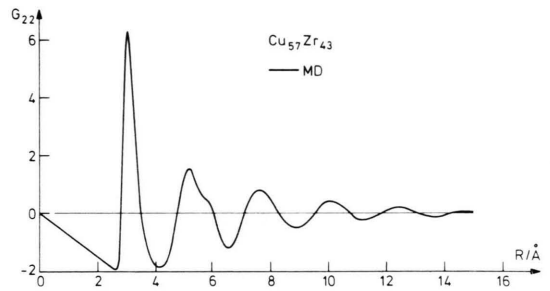

Fig. 6. As in Fig. 4, but $G_{\text{Zr-Zr}}(R)$.

other hand, the existing theoretical G_{ij}-functions exhibit peaks by a factor 2–3 too large [26] or have been cut at a hight of 4.0, so that a comparison with these curves is excluded [25], too.

5. Discussions and conclusions

The simulations of the $Cu_{57}Zr_{43}$ glass involve no severe problems due to the low reduced density and the small σ_{22}/σ_{11} quotient of the component-particles and the non-specific 1–2 interaction of the atoms. So we are convinced that the model G_{ij}-functions calculated at thermodynamic equilibrium of a fluid with a reduced temperature near 1, will fairly agree with the realistic G_{ij}-functions of the $Cu_{57}Zr_{43}$ metallic glass. Unfortunately as yet there are no realiable experimental G_{ij} to compare with.

Exactly from these points of view the $Ni_{81}B_{19}$ metallic glass proves difficult to be modelled as a fluid in a stationary state. The volume of the Ni-atoms is roughly by a factor of 3 greater than that of the B-atoms (see Table 1).

The reduced density of the Ni/B system is about 40% larger than that of normal liquid mixtures. For a liquid mixture of component-particles with very different sizes, the structure is essentially determined by the σ_{22}/σ_{11} ratio [29]. At a ratio of 2.0, for instance, the second peak of the PDF 1 vanishes for compositions where the particles of component 2 predominate [30]. Apparently the small particles were displaced by the much bigger particles, thus preventing them from forming a second coordination shell. However, at those reduced densities around 0.8 the smaller particles are not completely displaced by the larger ones, and a first coordination shell can nevertheless be built. Hitherto the first peak of the PDF 1 is still visible. In the case of the much larger reduced density of a metallic glass, the atoms with the small size are completely disjuncted by the large ones, and so the first coordination shell of the former disappears totally, a first peak of the G_{22} being not observed. However, simulating this system at a reduced temperature of roughly $T^* = 1$, the mobility of the involved particles, essentially of the small particles, is drastically enhanced resulting in a slight probability of finding small particles as nearest neighbours. Consequently, the simulation would generate a small 1st peak of the G_{22}-function in contrast to the measurements. To prevent the small particles (with their high kinetic energy) from forming a nearest neighbour shell we artificially enlarged the σ_{22}-parameter of the small atoms, here the B-atoms. The new σ_{BB}-parameter has a length which agrees roughly with the distance of two B-particles situated at the gaps between Ni-atoms. The schematic drawing of Fig. 7 shows this in a 2-dimensional model ($\sigma_{22} \approx 2 \cdot h/2^{1/6}$).

On the basis of this effective B-B "volume parameter", which accounts for the immobility of the B-particles in the glass, the calculated G_{ij}-functions have been obtained in accord with measured curves. It must be stressed again that all the other param-

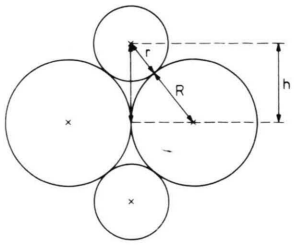

Fig. 7. Packing model for the $Ni_{81}B_{19}$-system.

eter have been left unchanged. The σ_{12}-parameter lies precisely at the Lorentz value if the original σ_{22}-parameter of B is accepted to be 1.586 Å (see Table 1). The small deviations of the higher order theoretical peaks from the experimental ones have to be a consequence of our introduced large σ_{22}-parameter. Because of this the model-system behaves less flexible than the experimental alloy. That means for the higher-order coordination shells, the Ni-atoms of the experimental system display a weaker tendency of displacing the B-atoms. Consequently the experimentally determined higher G_{22}-peaks migrate to lower distances, in contrast to the corresponding model peaks.

Summarizing we conclude the following facts

(i) MD provides model G_{ij}-functions on the basis of L-J (12-6) potentials which are in accordance with the measured G_{ij}-curves of metallic glasses.

(ii) A metallic glass resembles a mixture system at non-stationary thermodynamic conditions, its structure seems, however, to be essentially determined by its prior equilibrium state.

(iii) The differences in the structure of the alloy compared to that of a normal liquid are mainly due to the enormous difference in the reduced density and the σ_{22}/σ_{11} ratio of the volume parameters of the particles. Whereas in liquids ϱ^* scarcely exceeds 0.9 and σ_{22}/σ_{11} varies between 1 and 1.2, the ϱ^* parameter of metallic glasses is about 1.2 and σ_{22}/σ_{11} often reaches values of 1.6.

Acknowledgement

We thank Prof. Dr. Steeb for useful advices and discussions. The "Rechenzentrum der Ruhr-Universität Bochum" supplied us generously with computer-time on the Cyber-205 vector-machine. Moreover we are grateful to the "Deutsche Forschungsgemeinschaft" for financial support.

Appendix

Determination of the LJ-parameters from crystal data

For crystals without basis one finds for the cohesive energy E per particle

$$E = \tfrac{1}{2} \sum_{\boldsymbol{R}}^{0} \Phi(\boldsymbol{R}) = \tfrac{1}{2} \sum_{p=1}^{\infty} n_p \Phi(s_p a) .$$

Here $\sum_{\boldsymbol{R}}$ is the sum over the lattice vectors, $\Phi(\boldsymbol{R})$ the spherically symmetric pair potential, n_p the number of the p^{th} neighbors and s_p the distance to the p^{th} neighbors in units of the nearest-neighbor distance a. For the 12-6 L-J potential the cohesive energy is to be found by

$$E(a) = 2\varepsilon \left(\frac{\sigma}{a}\right)^6 \left[\left(\frac{\sigma}{a}\right)^6 S_{12} - S_6\right];$$

$$S_n = \sum_{p=1}^{\infty} \frac{n_p}{s_p^n} .$$

Inserting the equilibrium condition $\mathrm{d}E/\mathrm{d}a = 0$, one finds

$$\sigma = \left(\frac{S_6}{2S_{12}}\right)^{1/6} \cdot a \quad \text{and} \quad \varepsilon = -2S_{12}E/S_6^2 .$$

$S_6 = 14.45176$; $S_{12} = 12.13188$ for an fcc-lattice.

Number of nearest neighbors

A comparison of MD and experimental values for the system $Ni_{81}B_{19}$:

	r_{ij}^{theo}/Å	r_{ij}^{exp}/Å	Z_{ij}^{theo}	Z_{ij}^{exp}
Ni-Ni	2.51	2.52	10.6[a]	10.8
B-Ni	2.10	2.11	8.6	9.3
Ni-B	2.10	2.11	2.0	2.2
B-B	3.26	3.29	4.2	3.6
	4.04	4.02	3.2	3.7

Experimental data from [13].
[a] The same upper integration limit as in [13].

The number of nearest neighbors around an origin particle is defined here by integrating the radial distribution functions $g_{ij}(r)$ and weighting them by the corresponding mole fractions:

$$Z_{ij} = x_i \int_{R_{\min}}^{R_{\max}} 4\pi r^2 \varrho_0 g_{ij}(r)\,\mathrm{d}r;$$

ϱ_0 number density (for details see [13] or [3]).

[1] P. Duwez (Editor), Metallic Glasses, American Society for Metals, Metal Park, Ohio 1976.
[2] J. M. Ziman, Models of Disorder, Cambridge University Press 1979.
[3] Y. Waseda, The Structure of Non-Crystalline Materials, McGraw-Hill, New York 1980.
[4] H. Warlimont, Vacuumschmelze Hanau, Colloquy at Ruhr-Universität Bochum (21. 1. 1983).
[5] T. Mizoguchi, T. Kudo, and T. Irisawa, Proceedings of the 3. Int. Conf. on Rapidly Quenched Metals, Brighton 3. – 7. July 1978, Vol. II, page 384.
[6] E. Nold, Über die partiellen Strukturfaktoren und die Defektstruktur der amorphen Legierung $Fe_{80}B_{20}$, Dissertation Stuttgart 1981.
[7] E. Nold, P. Lamparter, H. Olbrich, G. Rainer-Harbach, and S. Steeb, Z. Naturforsch. **36a,** 1032 (1981).
[8] T. Fujiwara, H. S. Chen, and Y. Waseda, Z. Naturforsch. **37a,** 611 (1982).
[9] see [1] Page 106 and J. L. Finney, Proc. Roy. Soc., **A319,** 479 (1970).
[10] S. Takeuchi and S. Kobayashi, phys. stat. sol. (a) **65,** 315 (1981).
[11] D. S. Boudreaux, Phys. Rev. **B18,** 4039 (1978).
[12] S. Steeb, W. Sperl, and P. Lamparter, Institut von Laue-Langevin (Grenoble): Annex to the Annual Report 1981, p. 183.
[13] W. Sperl, Neutronen- und Röntgenbeugungsuntersuchungen an den metallischen Gläsern $Ni_{81}B_{19}$ und $Co_{80}P_{20}$, Dissertation Stuttgart 1982. – P. Lamparter, W. Sperl, S. Steeb, and J. Blétry, Z. Naturforsch. **37a,** 1223 (1982).
[14] T. Kudo, T. Mizoguchi, N. Watanabe, N. Niimura, M. Miswa, and K. Suzuki, J. Phys. Soc. Japan **45,** 1773 (1981).
[15] H. S. Chen and Y. Waseda, phys. stat. sol. (a) **51,** 593 (1979).
[16] J. P. Hansen and I. R. McDonald, Theory of Simple Liquids, Academic Press, London 1976.
[17] F. Vesely, Computerexperimente an Flüssigkeitsmodellen, Physik Verlag, Weinheim 1978.
[18] C. Hoheisel, Habilitationsschrift Bochum 1979, Phys. Chem. Liq. **9,** 245 (1980).
[19] D. Henderson and P. J. Leonard, Phys. Chem., An Advanced Treatise VIII B, Academic Press, New York 1971, p. 413.
[20] W. W. Wood in Phys. of Simple Liquids, Ed. H. N. V. Temperley, J. S. Rowlinson, and G. S. Rushbrooke, North-Holland Publishing Company, Amsterdam 1968.
[21] G. Sobotta and D. Wagner, Z. Physik **B33,** 271 (1979).
[22] G. Jacucci and I. R. McDonald, Mol. Phys. **27,** 1173 (1974).
[23] Y. Waseda and T. Masumoto, Z. Physik **B21,** 235 (1975), $\varrho = 7.382$ g cm^{-3}.
[24] Private communication from Mr. Hilzinger (VAC, Hanau), $\varrho = 7.51$ g cm^{-3}.
[25] S. Kobayashi, K. Maeda, and S. Takeuchi, J. Phys. Soc. Japan **48,** 1147 (1980).
[26] D. S. Boudreaux, Structure of Metallic Glass Alloy Research Report No. 80, Project 6003, November 1980, Allied Chemical Corporation.
[27] K. A. Gschneidner, Jr., Sol. State Physics **16,** 276 (1964), Editors: F. Seitz and D. Turnbull.
[28] Landolt-Börnstein, Zahlenwerke und Funktionen aus Wissenschaft und Technik, Ed.: K.-H. Hellwege, Neue Serie 1979; Springer-Verlag, Berlin.
[29] C. Hoheisel, Ber. Bunsenges. Phys. Chem. **85,** 1054 (1981).
[30] M. Schoen and C. Hoheisel, accepted in Mol. Phys. 1983.
[31] C. Kittel, Einführung in die Festkörperphysik, R. Oldenburg-Verlag, München 1973, page 62, 164.
[32] The bond length of B_2 is 1.589 Å see page F-217, CRC Handbook of Chemistry and Physics, 60th Edition 1979 – 1980 (Ed. R. C. Weast).
[33] For binary mixtures A_1/B_2 the larger atom radius is denoted by the σ_{22}-parameter. However, for the Ni/B system this convention is violated owing to the fact that the boron-radius is much smaller than the Ni-radius. But the calculations were based on a larger σ-parameter with respect to the B-B interaction. One has to pay attention to this, when the σ_{22}/σ_{11} ratio is discussed.